Light assisted solar fuel production by artificial CO_2 Reduction and water Oxidation

Deliverable D4.1

Summary of computational approaches & models

Lead Beneficiary:	ICFO
Delivery date:	28 February 2022
Dissemination level:	Public
Version:	v1.0

This Project has received funding from the European Union's Horizon 2020 research and innovation programme under grant agreement No. 951843

Document Information

Grant Agreement Number	951843
Acronym	LICROX
Start date of project (Duration)	01/09/2020 (36 months)
Document due date	28/02/2022
Submission date	28/02/2022
Authors	Catarina Ferreira, Jordi Martorell
Deliverable number	D4.1
Deliverable name	Summary of computational approaches & models
WP	WP4 – Light trapping in the PEC

Version	Date	Author	Description
v 0.1	25/02/2022	Catarina Ferreira (ICFO), Jordi Martorell (ICFO)	Creation first draft
v 1.0	28/02/2022	Laura Villar (ICIQ), Antoni Llobet (ICIQ), Laura López (ICIQ)	Final document following final revision and approval by the Project Management Board.

EXECUTIVE SUMMARY

This document, a public report on the computational approaches and models, is a deliverable of the LICROX Project, which is funded by the European Union's H2020 Programme under Grant Agreement No. 951843. It aims to expose in a detailed manner all the theoretical models used to study the light propagation inside the tandem photoelectrochemical cells, and in particular to determine the external quantum efficiency and short circuit currents of the different materials. In addition, it also presents some strategies applied to optimize the performance of the given tandem devices, both by introducing 1-dimensional nanophotonic structures and/or by using 3-dimensional scattering centers. Some main computational results are also presented and indicate that in both cases a considerable increase of the $BiVO_4$ short circuit current can be achieved in relation to a bare flat photoanode due to a better light trapping and distribution alongside the device.

Table of Contents

WP4: Light trapping in the PEC

In this WP4, the light propagation and absorption within the photoelectrochemical cells (PEC) are thoroughly studied, for both half and full PEC. Computational models are implemented to obtain the optimal 1-dimensional and 3-dimensional configurations, which ensure an optimal light distribution throughout the whole tandem and lead to an enhancement of the current density and consequent photocatalytic performance.

1. Purpose of the computational approaches and models

$BiVO_4$ is a high bandgap (nearly 2.5 eV) semiconductor[1], with a much smaller absorption range than the organic photovoltaic (OPV) cell and the photocathode that compose the tandem device. For this reason, the current generated by the photoanode will be lower than for the other two components and it will limit the whole monolithic device, when connected in series. This means that a large fraction of the current generated by the OPV cell will not be used by the tandem, especially when a half-cell is considered. Such issue can be solved both by implementing planar nanophotonic structures to ensure a proper light distribution among the different components of the tandem and by introducing light scattering centers to trap the light in the $BiVO_4$ photoanode, increasing the light path and enhancing the absorption without the need to increase the layer thickness (which is detrimental due to the increase in charge recombination). Both one-dimensional and three-dimensional models are necessary to describe the planar nanophotonic structures and the scattering centers, respectively.

2. 1-dimensional optimization of the PEC

For planar structures, the electric field propagation can be determined by solving the one-dimensional Maxwell equations through a general transfer-matrix method[2], that considers the coherent light propagation in the multilayer thin film stacks (photoanode, OPV cell and photocathode), as well as the incoherency introduced by the millimeter-thick glasses.

For a single stack with *f-1* thin layers illuminated only from the left side, as represented in Figure 1, the light propagation can be described by a single matrix $S_{0,f}$, which takes into account the change in electric field at the interface between two consecutive layers *j* and *k*, given by the matrix I_{jk}:

$$I_{j,k} = \frac{1}{t_{j,k}} \begin{bmatrix} 1 & r_{j,k} \\ r_{j,k} & 1 \end{bmatrix} \quad \text{(eq. 1)}$$

as well as the variations in electric field alongside a layer *j*, described by a propagation matrix, P_j:

$$P_j = \begin{bmatrix} e^{-ik_{jz}d_j} & 0 \\ 0 & e^{ik_{jz}d_j} \end{bmatrix} \quad \text{(eq. 2)}$$

In the previous equations, $r_{j,k}$ and $t_{j,k}$ are the Fresnel coefficients for the reflection and transmission of the light between two consecutive layers *j* and *k*, d_j the thickness of the layer *j* and k_{jz} the propagation vector in the z direction of the layer *j*, which is related to the complex refractive index $\tilde{n}_j = n_j + ik_j$ and to the angle of incidence of the light, θ_0.

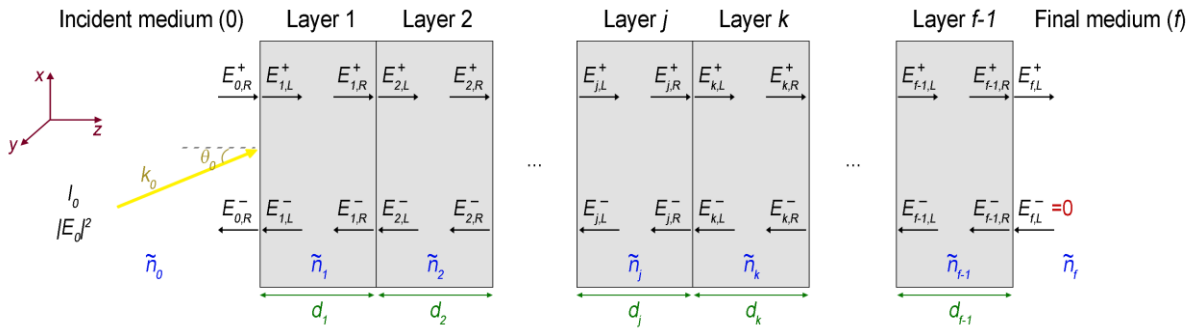

Figure 1. Multilayer stack with *f-1* thin layers parallel to each other, enclosed between an incident and a final medium, and with light impinging from the left side, as considered for the 1-dimensional transfer matrix calculations. The different refractive indexes and electric field components at each layer are also represented, following the same nomenclature used throughout the calculations.

The total matrix that relates the electric field in the right boundary of the incident medium, $E_{0,R}$, with the one in the left boundary of the final medium, $E_{f,L}$, is therefore given by:

$$S_{0,f} = \left(\prod_{j=1}^{f-1} I_{j-1,j}\, P_j \right) I_{f-1,f} \; ; \; \begin{bmatrix} E^+_{0,R} \\ E^-_{0,R} \end{bmatrix} = S_{0,f} \begin{bmatrix} E^+_{f,L} \\ E^-_{f,L} \end{bmatrix} \qquad \text{(eq. 3)}$$

Similar matrices can be written for the partial subsystems comprising all the layers between the incident medium and the left boundary of layer *j*, S_{0,j_L}, as well as the one containing all the layers between the right boundary of layer *j* and the final medium, $S_{j_R,f}$. Given that no light is able to enter the multi-stack from the final medium, $E^-_{f,L} = 0$ and the transmission coefficients between the incident medium and any layer *j*, t^+_{0,j_L} and t^-_{0,j_L}, can be easily determined. This allows the calculation of the electric field amplitude at any point *z* of the layer *j*, which for s-polarized light takes the form:

$$\begin{aligned} \left| E_j^{(s)}(z) \right|^2 = |E_0|^2 \Big[& \left| t^+_{0,j_L} \right|^2 e^{-2\mathbb{Im}(k_{jz})z} + \left| t^-_{0,j_L} \right|^2 e^{2\mathbb{Im}(k_{jz})z} \\ & + t^+_{0,j_L} \left(t^-_{0,j_L} \right)^* e^{2i\,\mathbb{Re}(k_{jz})z} + t^-_{0,j_L} \left(t^+_{0,j_L} \right)^* e^{-2i\,\mathbb{Re}(k_{jz})z} \Big] \end{aligned} \qquad \text{(eq. 4)}$$

The absorptance A_j at such layer *j*, for a given wavelength λ, is related with the optical power dissipation in the z direction, $Q_{jz}(z)$, which in turn depends on the electric field amplitude, such that:

$$A_j(\lambda) = \frac{\int_{d_{j-1}}^{d_j} Q_{jz}(z)\, dz}{I_0(\lambda)} = \frac{\int_{d_{j-1}}^{d_j} c\varepsilon_0 \mathbb{Im}(k_{jz}) \mathbb{Re}(k_{jz}) \left| E_j(z) \right|^2 dz}{k_0(\lambda)\, I_0(\lambda)} \qquad \text{(eq. 5)}$$

Finally, the short circuit current of the stack, J_{SC}, can be calculated by integrating the external quantum efficiency (EQE) over the range of wavelengths for which the active material absorbs, which in turn is proportional to the absorptance of the active layer:

$$J_{SC} = q \int \Phi(\lambda)\, \mathrm{EQE}(\lambda)\, d\lambda = q \int \Phi(\lambda)\, \eta_A\, A_j(\lambda)\, d\lambda \qquad \text{(eq. 6)}$$

In the equations above, c, ε_0 and q are physical constants corresponding to the speed of light, vacuum permittivity and elementary charge, $k_0(\lambda) = 2\pi/\lambda$ is the wave vector, $I_0(\lambda)$ is the incident irradiance, $\Phi(\lambda)$ is the photon flux at a given wavelength λ and η_A is the photon to charge conversion efficiency of the active material.

The equations above allow us to determine the properties of the photoanode, OPV cell and photocathode when they are individually considered. However, for a tandem device, the incident irradiances and electric field amplitudes $|E_0|^2$ depend on the total configuration of the tandem and need to be calculated. For that, a similar matrix method should be employed, but this time taking into account the changes in irradiance, instead of electric field. In this regard, the matrix that relates the irradiances before and after a given multi-stack *MS*, IRR_{MS}, is given by:

$$IRR_{MS} = \frac{1}{T_{MS}} \begin{bmatrix} 1 & -R_{MS} \\ R_{MS} & T_{MS}T'_{MS} - R_{MS}R'_{MS} \end{bmatrix} \quad \text{(eq. 7)}$$

where the different matrix elements are the total transmittance and reflectance of the multi-stack when illuminated from the front side (T_{MS}, R_{MS}) and the back side (T'_{MS}, R'_{MS}), and can easily be determined from eq. 3. On the other hand, for the thick glasses that separate the different stacks it is also possible to describe the variation in irradiance by a matrix IRR_G which depends on the absorption coefficient, α_G, and thickness of the glass, d_G:

$$IRR_G = \begin{bmatrix} e^{\alpha_G d_G} & 0 \\ 0 & e^{-\alpha_G d_G} \end{bmatrix} \quad \text{(eq. 8)}$$

In a similar way as before, we can write a single matrix that describes the behavior of the irradiance in the full tandem system, or in parts of the system, simply by multiplying all the matrices corresponding to the different multi-stacks and glasses, in the proper order. From that, one can easily get the irradiance that enters in a given thin layer stack *MS*, I_{MS}, which in turn is directly related to the electric field amplitude that enters in such multi-stack, $|E_{MS}|^2$:

$$|E_{MS}|^2 = \frac{k_{0z}\, I_{MS}}{k_{MSz}\, I_0} |E_0|^2 \quad \text{(eq. 9)}$$

With this general transfer matrix method, it is possible to determine all the optical properties of the full tandem configurations, and it can be applied both to the half and full PEC. In addition, the combination of this method with an optimization algorithm well suited to describe systems with a large number of variable parameters, which is the case of the genetic algorithm, allows for an inverse design optimization of the 1-dimensional nanophotonic structures. In this regard, a MATLAB® code was written to combine all the theoretical models and algorithms described above, in order to obtain the optimal structures for both the half cell and full cell configurations. While the first calculations have already been finalized, the latter are still ongoing and may be completed soon.

3. 3-dimensional optimization of the PEC

Even though a substantial improvement of the photoanode performance can be predicted by the use of 1-dimensional nanophotonic structures, such is limited by the planar nature of the configuration, in which the light rays can only perform a maximum of two passes inside the $BiVO_4$ layer. To further increase the photoanode J_{SC} above such limit, it is necessary to add 3-dimensional scattering centers to the PEC.

To address such problem, the Maxwell equations in the three-dimensional space need to be solved, which requires the implementation of numerical methods. In this particular case, we have chosen to use a finite element method, employed by means of COMSOL Multiphysics® software, in which a large system is subdivided into smaller, simpler parts that are called finite elements and which are modeled by simpler equations. In the preliminary study performed so far, cylindrical scatterers were placed on the surface of the

$BiVO_4$ photoanode, in contact with the water, as represented schematically in Figure 2 a). Periodic boundary conditions were established for the x and y directions (indicated in the figure) such that the unit cell is infinitely repeated in the xy plane, giving rise to a structure comprising an infinity of equally spaced cylindrical scatterers, which better simulates the experimental reality. In this case, only the photoanode can be considered, as the computational complexity and the time required to solve the electromagnetic equations are strongly dependent on the dimensions of the unit cell, which makes it unfeasible in terms of time and computational resources to model the full tandem system.

In a preliminary analysis, some of the main parameters of the problem were varied manually to get an estimate of the most favorable configuration of the scattering centers: refractive index of the scatterer, dimension (height and weight) of the cylinders, type of lattice (square or triangular, see Figure 2 b)) and periodicity. The best performance so far was obtained for a triangular array of 250nm radius x 250nm height TiO_2 cylinders with a lattice constant of 750nm. In such case, the EQE increased significantly for all wavelengths above 360nm, as shown in Figure 2 c), which resulted in a J_{SC} improvement of almost 22% in relation to the flat $BiVO_4$ photoanode, a value which should further increase when the OPV cell with a 1-dimensional nanophotonic structure is added.

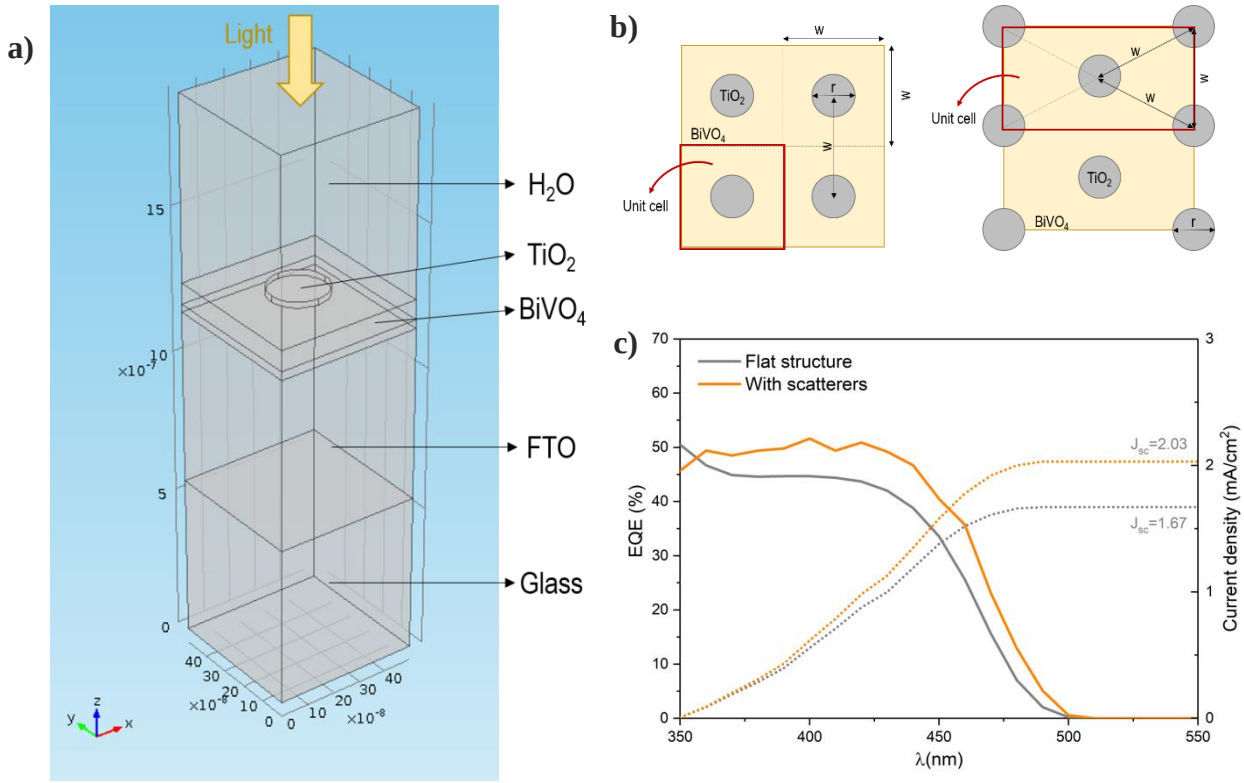

Figure 2. a) Unit cell considered for the 3-dimensional light absorption modeling problem, which includes the planar layers of the photoanode already considered for the 1-dimensional case and a cylindrical scatterer on top of the $BiVO_4$. b) Square (left) and triangular (right) lattices considered for the periodicity of the scattering centers. c) EQE and J_{SC} of the photoanode in a planar configuration (grey) and with cylinder scatterers (orange) with the best configuration found up to the moment placed on top of the $BiVO_4$ layer.

Ideally, to determine the optimal configuration of the scattering centers, an optimization algorithm well suited to describe the continuous structure of the light scatterers and compatible with the numerical methods used to solve the Maxwell equations in 3-dimensions, as is the case of the topology optimization or other gradient-based algorithm approaches, should be employed. However, until now we are still unsure if this approach is viable due to the computational effort required by the combination of both methods. In case we cannot proceed with such optimization, we will work to find the best possible structure in a more intuitively

fashion, by proving different shapes of the scattering centers and by sweeping the main parameters towards a maximization of the photoanode short circuit current.

4. References

1. Cooper, J. K. *et al.* Indirect bandgap and optical properties of monoclinic bismuth vanadate. *J. Phys. Chem. C* **119**, 2969–2974 (2015).
2. Katsidis, C. C. & Siapkas, D. I. General transfer-matrix method for optical multilayer systems with coherent, partially coherent, and incoherent interference. *Appl. Opt.* **41**, 3978–3987 (2002).